KINETIC RIEMANNIAN METRICS, LEVI-CIVITA CONNECTIONS, AND CURVATURE TENSORS ON LINKAGE CONFIGURATION SPACES

JEFFREY J. ROLLAND

Abstract. In geometric mechanics, the generalized mass (inertia) matrix $M(q)$ of an articulated multibody linkage induces a natural kinetic energy Riemannian metric $g = M(q)$ on the system's configuration manifold Q [1, 3]. This paper investigates the explicit metric tensors and their induced differential geometric structures—including the Levi-Civita connection (Christoffel symbols), Riemann curvature tensor, sectional/scalar curvatures, and invariant Riemannian volume forms—across open and closed kinematic chains [2, 4]. We evaluate the metric geometries of the spherical pendulum (S^2), the planar 2R robot arm (T^2), and closed-chain planar linkages whose configuration spaces form compact orientable surfaces of higher genus: the 5-bar mechanism (Σ_2, formed as the connected sum of two tori) and multi-loop coupled linkages (Σ_3, a genus-3 surface). Global geometric and topological invariants are verified using the Gauss–Bonnet theorem [2]. Accompanying parametric CAD assemblies and open-source symbolic verification scripts are provided.

1. Introduction

In Lagrangian mechanics, the kinetic energy T of an n-degree-of-freedom holonomic mechanism whose configuration is parameterized by local generalized coordinates $q = (q^1, \dots, q^n) \in U \subset Q$ is quadratic in the generalized velocities $\dot{q}$ [1, 5]:

$$T(q, \dot{q}) = \frac{1}{2}\dot{q}^T M(q)\dot{q} = \frac{1}{2} g_{ij}(q)\dot{q}^i\dot{q}^j, \tag{1}$$

where Einstein summation convention is assumed. The symmetric, positive-definite generalized mass matrix $M(q) = [g_{ij}(q)]$ endows the smooth configuration manifold Q with a natural Riemannian metric g [3].

Under this Riemannian formulation, unforced conservative motions correspond precisely to geodesics of the metric connection ∇ [1, 3]. The equations of motion take the geometric form [3]:

$$\nabla_{\dot{\gamma}}\dot{\gamma} = g^{\sharp}(F_{\text{ext}} - \text{grad}_g V), \tag{2}$$

Date: November 22, 2026.

2020 *Mathematics Subject Classification.* Primary 70B15, 53B20, 53Z05; Secondary 70G45, 57R19.

Key words and phrases. Riemannian metric, mass matrix, Christoffel symbols, Gaussian curvature, configuration space, 5-bar linkage, spherical pendulum, connected sum, higher-genus surface.

or in local coordinate components [4]:

$$\ddot{q}^i + \Gamma^i_{jk}(q)\dot{q}^j\dot{q}^k = g^{il}(q)Q_l, \tag{3}$$

where Γ^i_{jk} denote the Christoffel symbols of the second kind for the Levi-Civita connection ∇, and Q_l represents non-geodesic generalized forces (such as potential forces $-\partial V/\partial q^l$ and applied actuator torques) [3, 4].

While open-chain systems admit product-manifold configuration spaces such as tori $T^n = (S^1)^n$, closed kinematic loops impose algebraic constraints that fundamentally alter both the global topology and local curvature of the configuration manifold [4]. In this paper, we derive the explicit mass matrices, connection coefficients, and curvature expressions for four representative systems:

(1) The spherical pendulum ($Q \cong S^2$),
(2) The planar double pendulum ($Q \cong T^2$),
(3) The closed planar 5-bar mechanism ($Q \cong \Sigma_2 \cong T^2 \# T^2$), and
(4) The planar multi-loop coupled linkage ($Q \cong \Sigma_3 \cong \#_{i=1}^3 T^2$).

All models, parameters, and symbolic derivations are supported by Onshape CAD models and verification code in Python, MATLAB, and Wolfram Mathematica.

2. Derivative Structures of the Kinetic Metric

Let (Q, g) be an n-dimensional configuration manifold endowed with a smooth kinetic Riemannian metric $g = g_{ij}dq^i \otimes dq^j$ [2]. We denote the components of the inverse metric matrix by g^{ij}, such that $g_{ik}g^{kj} = \delta^j_i$.

Definition 1 (Metric Derivatives and Levi-Civita Connection)**.** *The Christoffel symbols of the first kind are defined by* [2]*:*

$$\Gamma_{ijk} = \frac{1}{2}\left(\frac{\partial g_{ik}}{\partial q^j} + \frac{\partial g_{jk}}{\partial q^i} - \frac{\partial g_{ij}}{\partial q^k}\right). \tag{4}$$

The Christoffel symbols of the second kind (the components of the symmetric Levi-Civita connection ∇) are [2]*:*

$$\Gamma^i_{jk} = g^{il}\Gamma_{jkl} = \frac{1}{2}g^{il}\left(\frac{\partial g_{lk}}{\partial q^j} + \frac{\partial g_{jl}}{\partial q^k} - \frac{\partial g_{jk}}{\partial q^l}\right). \tag{5}$$

In robotics and mechanism dynamics, the Coriolis and centrifugal matrix $C(q, \dot{q})$ is canonically assembled from the Christoffel symbols of the first kind via [4]:

$$C_{ij}(q, \dot{q}) = c_{ijk}(q)\dot{q}^k = \Gamma_{jik}(q)\dot{q}^k = \frac{1}{2}\left(\frac{\partial g_{ij}}{\partial q^k} + \frac{\partial g_{ik}}{\partial q^j} - \frac{\partial g_{jk}}{\partial q^i}\right)\dot{q}^k. \tag{6}$$

This construction guarantees that $\dot{M}(q) - 2C(q, \dot{q})$ is skew-symmetric, directly reflecting the metric compatibility condition $\nabla g = 0$ [3, 4].

Definition 2 (Curvature Tensors)**.** *The components of the Riemann curvature* $(3, 1)$*-tensor R are given in local coordinates by* [2]*:*

$$R^\rho{}_{\sigma\mu\nu} = \frac{\partial \Gamma^\rho_{\sigma\nu}}{\partial q^\mu} - \frac{\partial \Gamma^\rho_{\sigma\mu}}{\partial q^\nu} + \Gamma^\rho_{\lambda\mu}\Gamma^\lambda_{\sigma\nu} - \Gamma^\rho_{\lambda\nu}\Gamma^\lambda_{\sigma\mu}. \tag{7}$$

Lowering the contravariant index gives $R_{\kappa\sigma\mu\nu} = g_{\kappa\rho} R^{\rho}{}_{\sigma\mu\nu}$ [2]. *The Ricci curvature tensor is* $R_{\sigma\nu} = R^{\mu}{}_{\sigma\mu\nu}$, *and the scalar curvature is* $S = g^{\sigma\nu} R_{\sigma\nu}$ [2]. *For a 2-dimensional configuration space (*$\dim Q = 2$*), the Gaussian curvature* $K(q)$ *satisfies* [2]*:*

$$K(q) = \frac{R_{1212}}{\det(g_{ij})} = \frac{S(q)}{2}. \tag{8}$$

3. The Spherical Pendulum (S^2 Configuration Space)

Consider a spatial pendulum consisting of a rigid rod connected to ground via a frictionless ball-and-socket joint, parameterized by spherical coordinates $(\theta, \phi) \in (0, \pi) \times [0, 2\pi)$ [5].

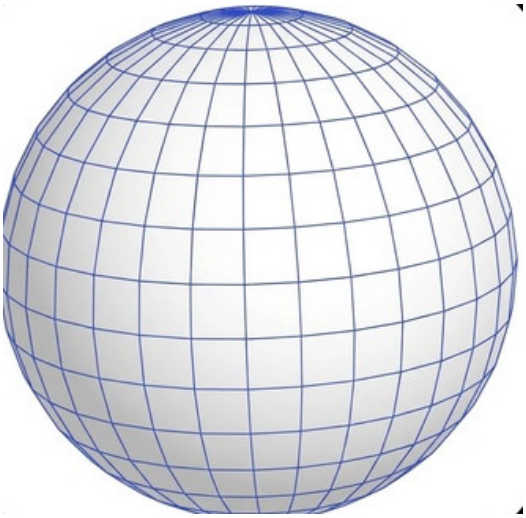

FIGURE 1. The regular 2-sphere S^2 as the configuration manifold of a spherical pendulum, endowed with coordinates (θ, ϕ) and constant positive Gaussian curvature $K = 1/J_O$.

3.1. Metric Tensor.

Let the total moment of inertia about the fixed origin O be J_O. For a rigid composite consisting of three components (attachment hub, cylindrical rod, and end bob):

$$J_O = \sum_{i=1}^{3} \left(I_{ci} + m_i r_{ci}^2 \right) = J_1 + J_2 + J_3. \tag{9}$$

The kinetic metric tensor takes the diagonal form [3]:

$$g(\theta, \phi) = \begin{bmatrix} J_O & 0 \\ 0 & J_O \sin^2 \theta \end{bmatrix}. \tag{10}$$

The CAD model for this mechanism is available in Onshape:

`https://cad.onshape.com/documents/602df2fb918a6b266b49b9ad`

For physical PLA prototyping values ($m_1 = 0.0052\,\mathrm{kg}$, $m_2 = 0.0106\,\mathrm{kg}$, $m_3 = 0.0419\,\mathrm{kg}$, length $l = 0.300\,\mathrm{m}$), the integrated inertia evaluates to $J_O = 4.0358 \times 10^{-3}\,\mathrm{kg}\cdot\mathrm{m}^2$.

3.2. **Connection Coefficients and Curvature.** The non-zero Christoffel symbols of the second kind are [2]:

$$\Gamma^{\theta}_{\phi\phi} = -\sin\theta\cos\theta, \tag{11}$$

$$\Gamma^{\phi}_{\theta\phi} = \Gamma^{\phi}_{\phi\theta} = \cot\theta. \tag{12}$$

The Gaussian curvature is constant [2]:

$$K = \frac{1}{J_O} > 0. \tag{13}$$

The Riemannian volume element is $d\mathrm{vol}_g = \sqrt{\det g}\, d\theta \wedge d\phi = J_O \sin\theta\, d\theta \wedge d\phi$. Integrating over S^2:

$$\oiint_{S^2} K\, d\mathrm{vol}_g = \int_0^{2\pi}\int_0^{\pi} \left(\frac{1}{J_O}\right) J_O \sin\theta\, d\theta\, d\phi = 4\pi = 2\pi\chi(S^2), \tag{14}$$

in agreement with the Gauss–Bonnet theorem [2].

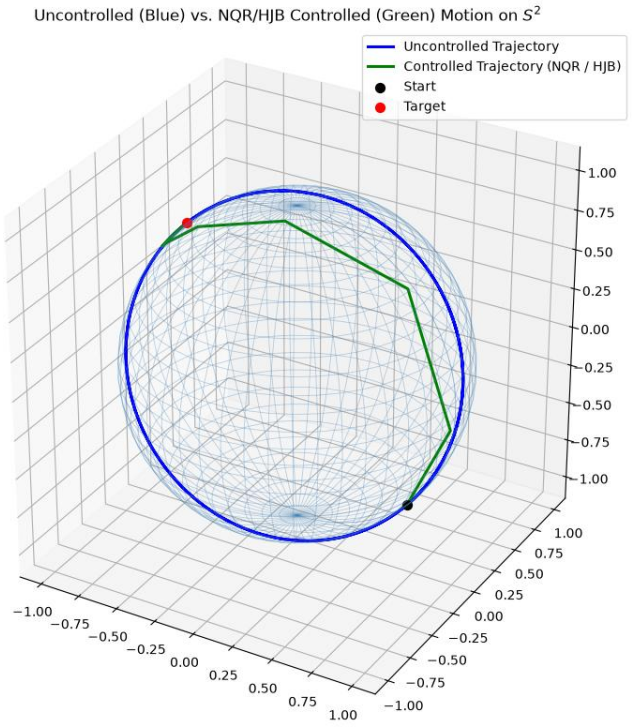

FIGURE 2. Comparison of uncontrolled geodesic motion (blue) and NQR/HJB controlled trajectories (green) on the spherical pendulum configuration manifold S^2.

4. The Planar Double Pendulum (T^2 Configuration Space)

Consider a planar two-link serial manipulator with joint angles $(\theta_1, \theta_2) \in [0, 2\pi)^2 \cong T^2$ [4].

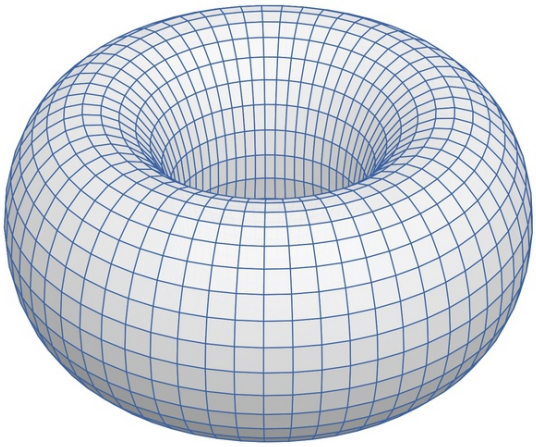

FIGURE 3. The 2-torus T^2 configuration manifold of a planar 2R double pendulum, admitting locally variable Gaussian curvature while possessing vanishing Euler characteristic $\chi(T^2) = 0$.

4.1. **Metric Tensor.** The kinetic metric tensor is given by [4]:

$$g(\theta_1, \theta_2) = \begin{bmatrix} a + b\cos\theta_2 & c + \frac{1}{2}b\cos\theta_2 \\ c + \frac{1}{2}b\cos\theta_2 & c \end{bmatrix}, \tag{15}$$

where

$$a = I_{zz,1} + I_{zz,2} + \frac{1}{4}m_1 L_1^2 + m_2 L_1^2 + \frac{1}{4}m_2 L_2^2, \tag{16}$$

$$b = 2L_1 r_{c2} m_2 = L_1 L_2 m_2, \tag{17}$$

$$c = I_{zz,2} + \frac{1}{4}m_2 L_2^2. \tag{18}$$

The CAD model and 3D print specifications are hosted at:

`https://cad.onshape.com/documents/fa6e8c4e48a0b023ac4fe14e`

For nominal experimental parameters ($m_1 = m_2 = 0.181\,\text{kg}$, $L_1 = L_2 = 0.250\,\text{m}$, $I_{zz,i} = 1.0 \times 10^{-3}\,\text{kg}\cdot\text{m}^2$):

$$g(\theta_1, \theta_2) = \begin{bmatrix} 0.0113\cos\theta_2 + 0.0190 & 0.00566\cos\theta_2 + 0.00383 \\ 0.00566\cos\theta_2 + 0.00383 & 0.00383 \end{bmatrix} \text{kg}\cdot\text{m}^2. \tag{19}$$

4.2. **Connection and Curvature.** Because the metric coefficients depend solely on the relative coordinate θ_2, all derivatives with respect to θ_1 vanish ($\partial g_{ij}/\partial\theta_1 = 0$) [4]. The non-zero metric derivatives are:

$$\frac{\partial g_{11}}{\partial\theta_2} = -b\sin\theta_2, \quad \frac{\partial g_{12}}{\partial\theta_2} = -\frac{1}{2}b\sin\theta_2, \quad \frac{\partial g_{22}}{\partial\theta_2} = 0. \tag{20}$$

Computing the Christoffel symbols of the first kind yields [4]:

$$\Gamma_{112} = \Gamma_{121} = -\frac{1}{2} b \sin\theta_2, \quad \Gamma_{211} = \frac{1}{2} b \sin\theta_2, \quad \Gamma_{122} = \Gamma_{222} = 0. \tag{21}$$

The determinant is $D(\theta_2) = \det g = ac - c^2 - \frac{1}{4} b^2 \cos^2\theta_2$. The Gaussian curvature evaluates to:

$$K(\theta_2) = \frac{b\, c^2 \left(4a \cos\theta_2 + b(1 + \sin^2\theta_2)\right)}{4 \left[ac - c^2 - \frac{1}{4} b^2 \cos^2\theta_2\right]^2}. \tag{22}$$

Although $K(\theta_2)$ is locally non-zero, the total curvature vanishes in accordance with the Gauss–Bonnet theorem [2]:

$$\oiint_{T^2} K \, d\mathrm{vol}_g = \int_0^{2\pi} \int_0^{2\pi} K(\theta_2) \sqrt{D(\theta_2)} \, d\theta_1 \, d\theta_2 = 2\pi \chi(T^2) = 0. \tag{23}$$

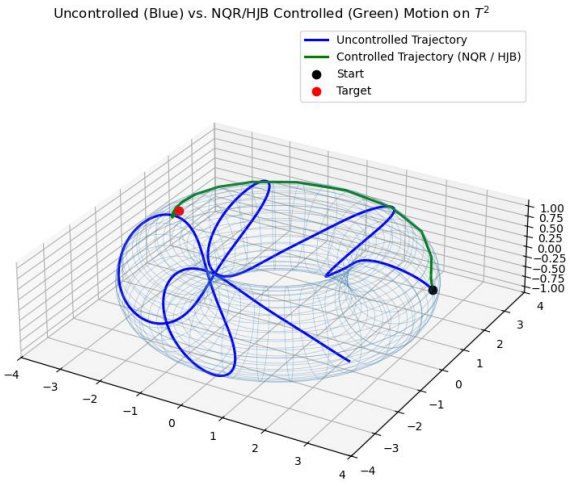

FIGURE 4. Comparison of uncontrolled motion (blue) and NQR/HJB controlled trajectories (green) on the 2-torus T^2 configuration space of the planar double pendulum.

5. The Planar 5-Bar Mechanism (Σ_2 Configuration Space)

When two 2R serial linkages are coupled at their endpoints to form a closed kinematic loop, the system constitutes a planar 5-bar mechanism [4]. The configuration space is the connected sum of two tori:

$$Q \cong T^2 \# T^2 \cong \Sigma_2, \tag{24}$$

a compact Riemann surface of genus $g = 2$.

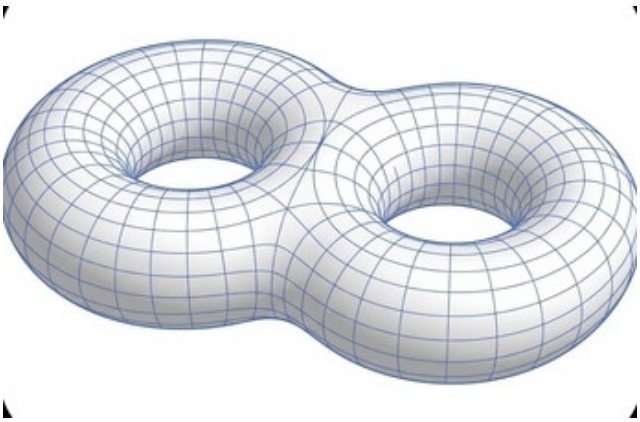

FIGURE 5. The genus-2 orientable surface $\Sigma_2 \cong T^2 \# T^2$ representing the configuration space of the closed-loop planar 5-bar linkage, with negative total Euler characteristic $\chi(\Sigma_2) = -2$.

5.1. **Parametrization and CAD Synthesis.** The Onshape kinematic assembly is provided at:

`https://cad.onshape.com/documents/30538255325c616d7151aa1d`

Let l_1, l_2, l_3, l_4 denote the moving link lengths, and l_5 denote the fixed ground link. Selecting the driven crank angles (θ_1, θ_4) as generalized coordinates on a regular chart, the passive angles θ_2 and θ_3 are determined by the vector loop-closure constraint [4]:

$$l_1 e^{i\theta_1} + l_2 e^{i\theta_2} - l_3 e^{i\theta_3} - l_4 e^{i\theta_4} - l_5 = 0. \tag{25}$$

5.2. **Reduced Metric Formulation.** Projecting the kinetic energy of the four moving links onto the independent velocities $(\dot{\theta}_1, \dot{\theta}_4)$ via the loop constraint Jacobian yields the reduced metric [3, 4]:

$$g(\theta_1, \theta_4) = \frac{1}{\sin^2(\theta_2 - \theta_3)} \begin{bmatrix} N_{11} & N_{14} \\ N_{14} & N_{44} \end{bmatrix}, \tag{26}$$

where

$$N_{11} = C_{12}\cos(2\theta_1 - 2\theta_2) + C_{13}\cos(2\theta_1 - 2\theta_3) + C_{23}\cos(2\theta_2 - 2\theta_3) + C_0, \tag{27}$$

$$N_{44} = C_{23}\cos(2\theta_2 - 2\theta_3) + C_{24}\cos(2\theta_2 - 2\theta_4) + C_{34}\cos(2\theta_3 - 2\theta_4) + C_0, \tag{28}$$

$$N_{14} = S_{12}\sin(\theta_1 - \theta_2)\sin(\theta_2 - 2\theta_3) + S_{34}\sin(\theta_3 - \theta_4)\sin(\theta_1 - 2\theta_2 + \theta_3), \tag{29}$$

and the structural inertia constants are:

$$C_{12} = -\frac{1}{2}\left(m_2 r_{c2}\frac{l_1^2}{l_2} + J_3\frac{l_1^2}{l_3^2}\right), \qquad C_{13} = \frac{1}{2}\left(m_2 r_{c2}\frac{l_1^2}{l_2} - J_2\frac{l_1^2}{l_2^2}\right), \tag{30}$$

$$C_{34} = -\frac{1}{2}\left(m_3 r_{c3}\frac{l_4^2}{l_3} + J_2\frac{l_4^2}{l_2^2}\right), \qquad C_{24} = \frac{1}{2}\left(m_3 r_{c3}\frac{l_4^2}{l_3} - J_3\frac{l_4^2}{l_3^2}\right), \tag{31}$$

$$C_{23} = -\frac{1}{2}\left(J_1 + m_2 l_1^2 - m_2 r_{c2}\frac{l_1^2}{l_2}\right), \qquad C_0 = -C_{23} + \frac{1}{2}\left(J_2\frac{l_1^2}{l_2^2} + J_3\frac{l_1^2}{l_3^2}\right), \tag{32}$$

$$S_{12} = -m_3 r_{c3}\frac{l_1}{l_3}, \qquad S_{34} = m_2 r_{c2}\frac{l_4}{l_2}. \tag{33}$$

5.3. **Numerical Implementation and Topological Verification.** For nominal prototype parameters ($m_1 = m_4 = 0.08697\,\mathrm{kg}$, $m_2 = 0.18072\,\mathrm{kg}$, $m_3 = 0.17969\,\mathrm{kg}$, $l_1 = l_4 = 0.100\,\mathrm{m}$, $l_2 = l_3 = l_5 = 0.250\,\mathrm{m}$), the evaluated kinetic metric takes the form:

$$g(\theta_1, \theta_4) = \frac{10^{-4}}{\sin^2(\theta_2 - \theta_3)}\begin{bmatrix}\hat{N}_{11} & \hat{N}_{14}\\ \hat{N}_{14} & \hat{N}_{44}\end{bmatrix}\ \mathrm{kg}\cdot\mathrm{m}^2, \tag{34}$$

where the dimensionless numerical numerators are given explicitly by:

$$\hat{N}_{11} = -7.818\cos(2\theta_1 - 2\theta_2) + 1.218\cos(2\theta_1 - 2\theta_3) - 6.405\cos(2\theta_2 - 2\theta_3) + 13.006, \tag{35}$$

$$\hat{N}_{44} = -6.405\cos(2\theta_2 - 2\theta_3) + 1.218\cos(2\theta_2 - 2\theta_4) - 7.818\cos(2\theta_3 - 2\theta_4) + 13.006, \tag{36}$$

$$\hat{N}_{14} = -8.984\sin(\theta_1 - \theta_2)\sin(\theta_2 - 2\theta_3) + 9.088\sin(\theta_3 - \theta_4)\sin(\theta_1 - 2\theta_2 + \theta_3). \tag{37}$$

The total integral of the Gaussian curvature across the regular configuration manifold Σ_2 is governed by its Euler characteristic $\chi(\Sigma_2) = 2 - 2(2) = -2$ via the Gauss–Bonnet theorem [2]:

$$\oiint_{\Sigma_2} K\, d\mathrm{vol}_g = 2\pi\chi(\Sigma_2) = 2\pi(-2) = -4\pi. \tag{38}$$

The numerical integration, Christoffel symbol computations, and dynamic simulation routines are implemented in the author's open repository:

`https://github.com/DeadbeatJeff/genus2TorusControlLaw`

6. Generalization to the Genus-3 Torus and the Arbitrary Genus-g Induction

The connected-sum construction formulated for the 5-bar linkage ($\Sigma_2 \cong T^2 \# T^2$) serves as the fundamental inductive step for multi-loop coupled linkages [3]. By chaining serial linkages through mutual closed loops, the genus-3 configuration space Σ_3 provides the key structural archetype for establishing the metric and topological properties of an arbitrary genus-g orientable surface Σ_g.

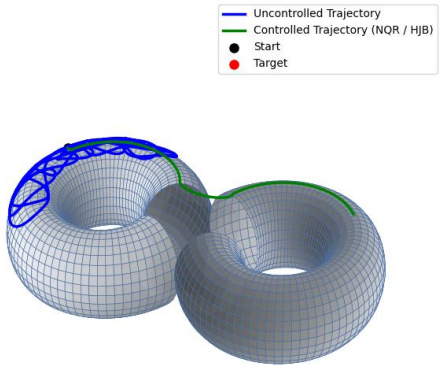

FIGURE 6. Comparison of uncontrolled motion (blue) and NQR/HJB controlled trajectories (green) across the genus-2 surface Σ_2 representing the closed-loop planar 5-bar linkage.

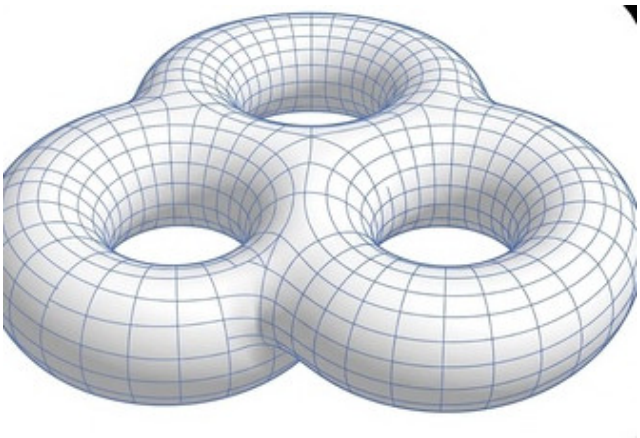

FIGURE 7. The genus-3 configuration manifold $\Sigma_3 \cong \#_{i=1}^{3} T^2$ arising from three coupled 2R kinematic loops, establishing the topological induction template for arbitrary genus-g systems.

6.1. **Topological Connected Sums and the Genus-g Archetype.** Coupling three 2R serial chains across two independent closed kinematic constraints yields a mechanism whose regular configuration manifold is the connected sum of three tori:

$$Q \cong T^2 \# T^2 \# T^2 \cong \Sigma_3. \tag{39}$$

The parametric CAD assembly of this coupled multi-loop mechanism is provided in Onshape:

`https://cad.onshape.com/documents/797c0a7c10a7ed01d84b041f`

More generally, an articulated planar linkage consisting of g coupled 2R loops subject to mutual closure constraints yields a configuration manifold topologically homeomorphic to a compact, orientable Riemann surface of genus g:

$$Q \cong \underbrace{T^2 \# T^2 \# \cdots \# T^2}_{g \text{ copies}} \cong \Sigma_g \cong \#_{i=1}^{g} T^2. \tag{40}$$

6.2. **Atlas Construction and Metric Volume Partitioning.** Because a surface of genus $g \geq 2$ cannot be covered globally by a single non-singular coordinate chart, the kinetic Riemannian metric g must be formulated on an atlas of charts reflecting the constituent loops [2].

For the genus-3 system, selecting independent coordinate pairs—such as (θ_1, θ_4) and (θ_1, θ_6), representing the driven base cranks of adjacent loops—partitions the total Riemannian volume across local coordinate patches $\Sigma_{3,1}$ and $\Sigma_{3,2}$ modulo transition boundaries:

$$\mathrm{Vol}_g(\Sigma_3) = \iint_{\Sigma_{3,1}} \sqrt{\det g(\theta_1, \theta_4)}\, d\theta_1 \wedge d\theta_4 + \iint_{\Sigma_{3,2}} \sqrt{\det g(\theta_1, \theta_6)}\, d\theta_1 \wedge d\theta_6. \tag{41}$$

Inductively, this establishes the general prescription for a genus-g mechanism: the global metric volume decomposes into the sum of Riemannian integrals over $g-1$ coupled charts covering the unconstrained kinematic varieties:

$$\mathrm{Vol}_g(\Sigma_g) = \sum_{k=1}^{g-1} \iint_{\Sigma_{g,k}} \sqrt{\det g_{(k)}(q_{(k)})}\, dq^1_{(k)} \wedge dq^2_{(k)}. \tag{42}$$

6.3. **Global Curvature and the Topological Invariant.** While the local metric tensor components g_{ij} and Christoffel symbols vary continuously with individual link masses, lengths, and inertia parameters, the total integrated Gaussian curvature across the regular configuration manifold is a strict topological invariant [2].

Applying the Gauss–Bonnet theorem to the genus-3 mechanism yields ($\chi(\Sigma_3) = 2 - 2(3) = -4$) [2]:

$$\oiint_{\Sigma_3} K\, d\mathrm{vol}_g = 2\pi\chi(\Sigma_3) = 2\pi(2 - 2(3)) = -8\pi. \tag{43}$$

This serves as the template for the general genus-g linkage configuration space:

$$\oiint_{\Sigma_g} K\, d\mathrm{vol}_g = 2\pi\chi(\Sigma_g) = 4\pi(1 - g). \tag{44}$$

The symbolics, automated multi-patch atlas calculations, and numerical curvature solvers for the genus-3 configuration space are maintained in the author's open repository:

`https://github.com/DeadbeatJeff/genus3ControlLaw`

For all higher-genus mechanisms ($g \geq 2$), the average Gaussian curvature $\langle K \rangle = \frac{4\pi(1-g)}{\mathrm{Vol}_g(\Sigma_g)}$ is strictly negative, reflecting hyperbolic metric behavior on large subsets of the configuration space [2]. Kinematic singular configurations—where loop-closure Jacobians degenerate or link alignments collapse ($\det g \to 0$ or $\sin(\Delta\theta) \to 0$)—correspond

to metric singularities delineating boundary components of the physical configuration charts within the ambient smooth manifold Σ_g [3, 4].

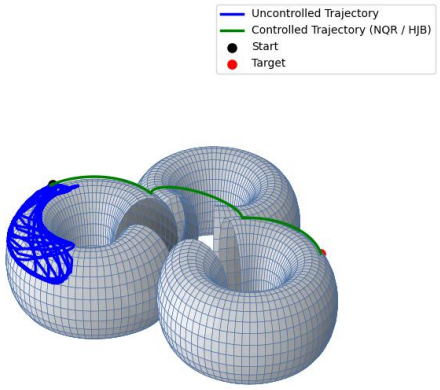

FIGURE 8. Comparison of uncontrolled motion (blue) and NQR/HJB controlled trajectories (green) across the genus-3 configuration manifold Σ_3.

REFERENCES

[1] V. I. Arnold. *Mathematical Methods of Classical Mechanics*. Graduate Texts in Mathematics, Vol. 60, Springer-Verlag, New York, 2nd edition, 1989.
[2] M. P. do Carmo. *Riemannian Geometry*. Birkhäuser, Boston, MA, 1992.
[3] F. Bullo and A. D. Lewis. *Geometric Control of Mechanical Systems: Modeling, Analysis, and Design for Simple Mechanical Control Systems*. Texts in Applied Mathematics, Vol. 49, Springer-Verlag, New York, 2005.
[4] R. M. Murray, Z. Li, and S. S. Sastry. *A Mathematical Introduction to Robotic Manipulation*. CRC Press, Boca Raton, FL, 1994.
[5] J. E. Marsden and T. S. Ratiu. *Introduction to Mechanics and Symmetry*. Texts in Applied Mathematics, Vol. 17, Springer-Verlag, New York, 2nd edition, 1999.

ALEXANDRIA, VA
Email address: jeffrey.rolland@mcdean.com